Progress In Electromagnetics Research Letters, Vol. 66, 25–31, 2017

A Wideband Circularly Polarized Slot-Loaded Dipole Antenna with L-Shaped Arms and Parasitic Patches

Wei Hu[1, *], Le-Hu Wen[1], Zhao-Yang Tang[1], Min Zhang[2], and Wen-Chao Xiao[2]

Abstract—In this paper, a broadband circularly polarized (CP) antenna based on slot-loaded dipole with L-shaped arms and parasitic patches is proposed and investigated. Circular polarization is initially obtained at the lower frequency by bending the dipole arms into L-shape. To extend the axial ratio (AR) bandwidth, two pairs of parasitic patches are introduced along the orthogonal sections of the L-shaped arms, so that the modified dipole can yield two additional minimum AR points at the center and higher frequency respectively. Meanwhile, to further extend impedance bandwidth and improve CP performance, circular slots are symmetrically embedded into the tapered-end of each arm design. The measured results of the antenna exhibit a 3-dB AR bandwidth of 61.3% within 10-dB return loss bandwidth of 64.0%. Besides, desirable gains across the wide operation band are also demonstrated.

1. INTRODUCTION

Circularly polarized (CP) antennas are highly desirable for modern wireless communication, because they can suppress multi-path interference and reduce polarization mismatch between transmitting and receiving antennas. The conventional microstrip antenna is often adopted to realize CP operation owing to its advantages of low profile and easy fabrication [1–4]. However, inherently narrow axial ratio (AR) bandwidth limits its availability in wideband CP applications, especially for the single-fed CP microstrip antennas [3, 4]. To improve the AR bandwidth, many effective approaches have been demonstrated and discussed by researchers. In the design presented in [5], cross-dipoles with metal vias and branches are employed to achieve a 3-dB AR bandwidth of 29.0%. In [6], by introducing overlapping square slot-rings, the antenna can yield a 3-dB AR bandwidth of 33% and a 10-dB impedance bandwidth of 53% with bi-directional radiation. Besides, by truncating a corner of the radiation patch, orthogonal modes of the L-shaped slot are induced to excite CP wave [7]. As a result, the antenna exhibits a 3-dB AR bandwidth of 47.8%. Unfortunately, these antennas [6, 7] with good AR bandwidth of over 30% have poor radiation patterns due to their asymmetric structures. Furthermore, some wideband CP antennas with various feeding networks are reported in [8, 9]. Unfortunately, their structures are complicated for the engineering applications.

Unlike the traditional CP crossed dipoles, in our previous study [10], a pair of parasitic strips had been properly introduced in a Z-shaped dipole antenna to obtain wideband CP characteristic. In this paper, the other pair of parasitic patches evolved from the previous work is utilized to generate an additional minimum AR point covering the upper operating band. Moreover, symmetrical circular slots are embedded in the dipole to improve impedance matching and CP performance. The measured results show the proposed antenna achieves a 3-dB AR bandwidth of 61.3%, which is increased by 20% compared with the previous study in [10]. The paper extends the previous study and provides an effective method for designing broadband circularly polarized antennas based on single-fed dipole and parasitic patches.

Received 11 January 2017, Accepted 3 February 2017, Scheduled 7 February 2017

* Corresponding author: Wei Hu (mwhuwei@163.com).

[1] National Laboratory of Science and Technology on Antennas and Microwaves, Xidian University, Xi'an, Shaanxi 710071, China. [2] Wuhan Maritime Communication Research Institute, Wuhan, Hubei 430079, China.

2. ANTENNA CONFIGURATION AND DESIGN

The geometry of the proposed CP antenna is shown in Figure 1. The antenna comprises a slot-loaded dipole with L-shaped arms, two pairs of parasitic patches marked as P_a and P_b, a printed balun and a ground plane. The modified dipole and parasitic patches are etched on the bottom of a 0.6 mm-thick FR4 substrate, which is placed horizontally with a size of $121 \times 121\,\text{mm}^2$. Tapered-shaped design is employed in the front-end of each dipole arm to realize the impedance matching over a wide operating band. As depicted in Figure 1(c), the feeding balun is composed of a Γ-shaped microstrip line and two rectangular strips, which are printed on a FR4 substrate placed vertically with a dimension of $60 \times 30 \times 1\,\text{mm}^3$. The two ends of the rectangular strip are connected to the dipole and the ground. All the FR4 substrates in the design have a relative permittivity of 4.4 and a dielectric loss tangent of 0.02. The antenna is placed above a reflecting ground whose size is $170 \times 170\,\text{mm}^2$. The SMA connector is mounted under the ground and its outer conductor is fixed on the ground plane. In addition, the detailed design parameters given in Figure 1 are $L_1 = 42\,\text{mm}$, $W_1 = 22\,\text{mm}$, $L_2 = 58\,\text{mm}$, $W_2 = 16\,\text{mm}$, $L_3 = 13\,\text{mm}$, $W_3 = 7\,\text{mm}$, $L_a = 33\,\text{mm}$, $W_a = 15\,\text{mm}$, $g_a = 2\,\text{mm}$, $L_b = 33\,\text{mm}$, $W_b = 15\,\text{mm}$, $g_b = 2\,\text{mm}$, $s = 18.5\,\text{mm}$, $D_s = 9\,\text{mm}$, $R_s = 4.2\,\text{mm}$, $D_f = 3\,\text{mm}$, $G_f = 9\,\text{mm}$, $L_{f1} = 6\,\text{mm}$, $W_{f1} = 1.9\,\text{mm}$, $L_{f2} = 12\,\text{mm}$, $W_{f2} = 0.8\,\text{mm}$, $L_{f3} = 16.8\,\text{mm}$, $L_{f4} = 10.4\,\text{mm}$, and $H = 30\,\text{mm}$.

Various structures involved in the evolution process of the wideband CP antenna design are presented in Figures 2 and 3. All simulations were performed by ANSYS HFSS. Ant. 1 in Figure 2 is a printed dipole whose arms are bent into L-shape for CP operation at first. This simple design, as shown in Figure 3, acquires a 3-dB AR band of 22.2% (1.80–2.25 GHz) within an effective impedance matching band. Then, in the design of Ant. 2, a pair of parasitic rectangular patches (P_a) is introduced along the x-directed section of the dipole arms to produce an additional minimum AR point at 2.7 GHz and achieve a better impedance match around 2.8 GHz. Figure 3 shows Ant. 2 has a 3-dB AR bandwidth

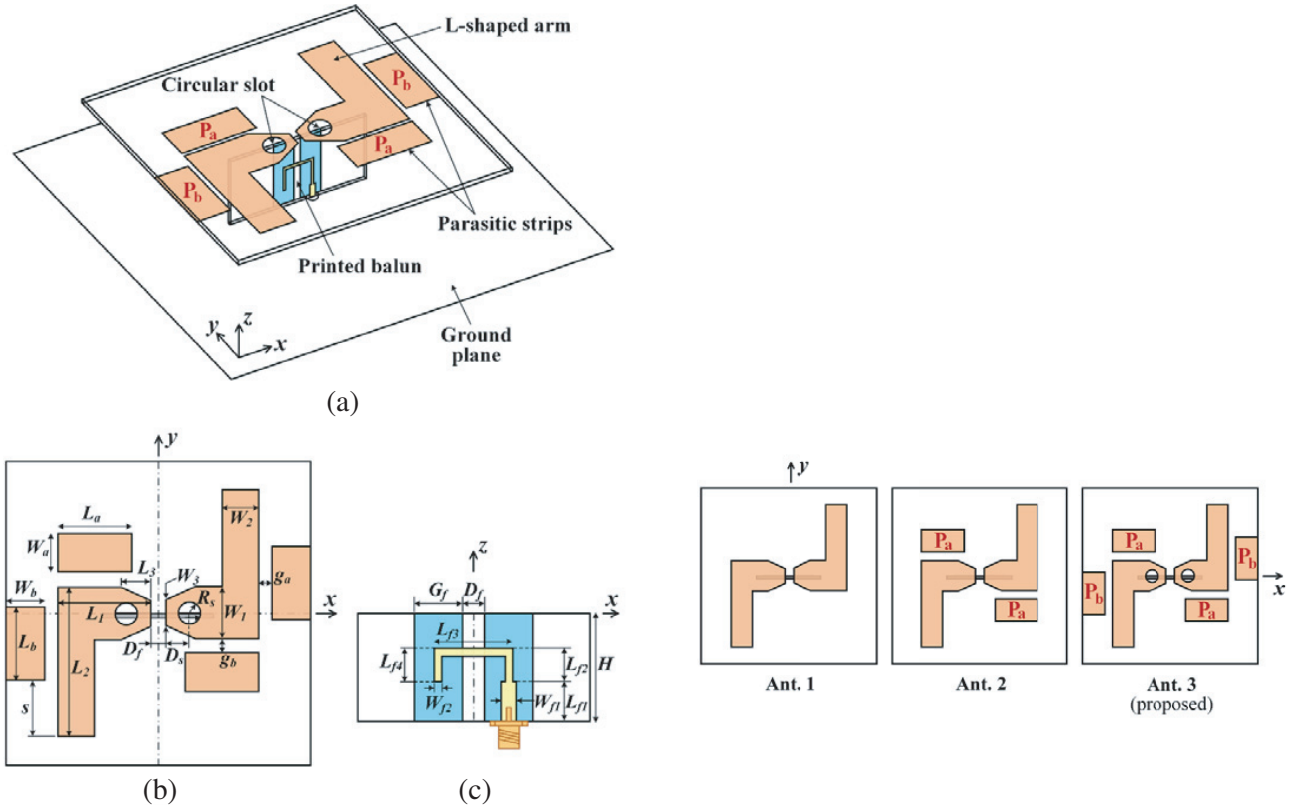

Figure 1. Geometry of the proposed antenna: (a) 3D view, (b) top view, (c) printed balun.

Figure 2. Various structures involved in the evolution process of the proposed antenna.

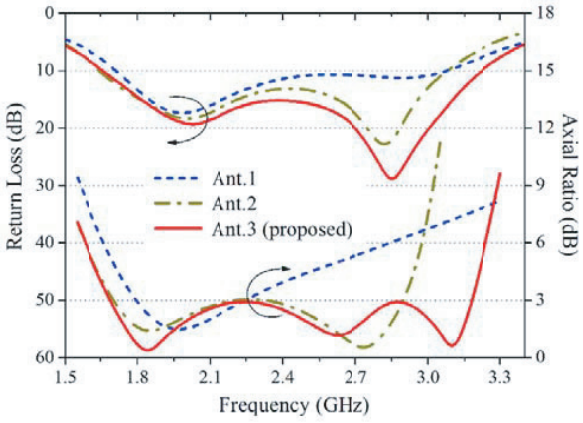

Figure 3. Simulated return loss and axial ratio of various antennas involved.

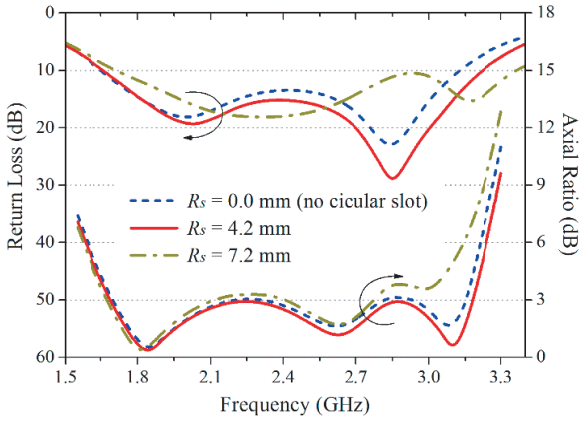

Figure 4. Effects of the slot radius R_s on return loss and axial ratio.

of 52.5% (1.70–2.91 GHz), with the impedance bandwidth wider than it. Next, to further increase the AR bandwidth, the other pair of parasitic patches (P_b) is placed along the y-directed section of the L-shaped arms in Ant. 3. Meanwhile, two circular slots are symmetrically embedded into the tapered-end of each arm to enhance impedance bandwidth and improve CP performance. In this way, it is clearly seen that one more additional minimum AR point can be obtained at 3.1 GHz. The simulated results of Ant. 3 exhibit a 3-dB AR bandwidth of 62.6% (1.67–3.19 GHz) within 10-dB return loss bandwidth of 64.5% (1.65–3.22 GHz). Lastly, Ant. 3 is the final antenna in this design, whose dimensions are given in Figure 1.

As shown in Figure 4, when adjusting the radius R_s of two circular slots loaded into the dipole arm, it is found that both the impedance matching in the upper band and the CP performance at third minimum AR point can be improved. While $R_s = 4.2$ mm, the widest CP and impedance operating bandwidths are achieved simultaneously.

In the design process of the proposed antenna, by bending the dipole arms into L-shape, circular polarization can be firstly obtained at the lower frequency. Then, the length L_a of parasitic patch P_a should be chosen in the important place because it can produce a minimum AR point at the center frequency. Next, by selecting an appropriate distance s from the end of the dipole arm to P_b, the CP operating band at the higher frequency can be achieved. Finally, the radius R_s of circular slot is tuned to further enhance impedance bandwidth and improve CP performance.

To analyze the mechanism for CP operation, the simulated surface current distributions on the slot-loaded dipole and parasitic patches at the three minimum AR points are illustrated in Figure 5. Note that a solid black arrow below each plot represents the sum of all major current contributions. At 1.8 GHz, most of the currents concentrate along the dipole arms. As depicted in Figure 5(a), it is obvious that the predominant surface current is mostly towards the $+x$ axis at phase of 0°, and towards $+y$ axis at phase of 90°. Thereby, the current on the slot-loaded dipole travels in the anticlockwise direction as phase increases, generating a right-hand circularly polarized (RHCP) radiation at the first AR point. At 2.6 GHz, the surface current distributions become concentrated on both the dipole and P_a, as shown in Figure 5(b). The resultant current at phase = 0° consists of the $-x$-directed current along dipole arms and $+y$-directed current along P_a. At phase of 90°, the resultant current is orthogonal to that at 0°, and rotates anticlockwise as phase increases. Thus, RHCP radiation is generated in the $+z$ direction at the second AR point. At 3.1 GHz, it is observed from Figure 5(c) that at phase of 0°, the surface currents are mainly distributed around P_a towards $+x$ axis and P_b towards $+y$ axis. The resultant current at phase = 0° is orthogonal to that at phase = 90°, which is composed of the $-x$-directed current along L-shaped arms and $+y$-directed current along P_b. As phase increases the resultant current rotates anticlockwise to generate RHCP radiation. From the above analysis, we can draw the conclusion that the third AR minimum point is determined by the dipole and all the parasitic patches (P_a and P_b) together.

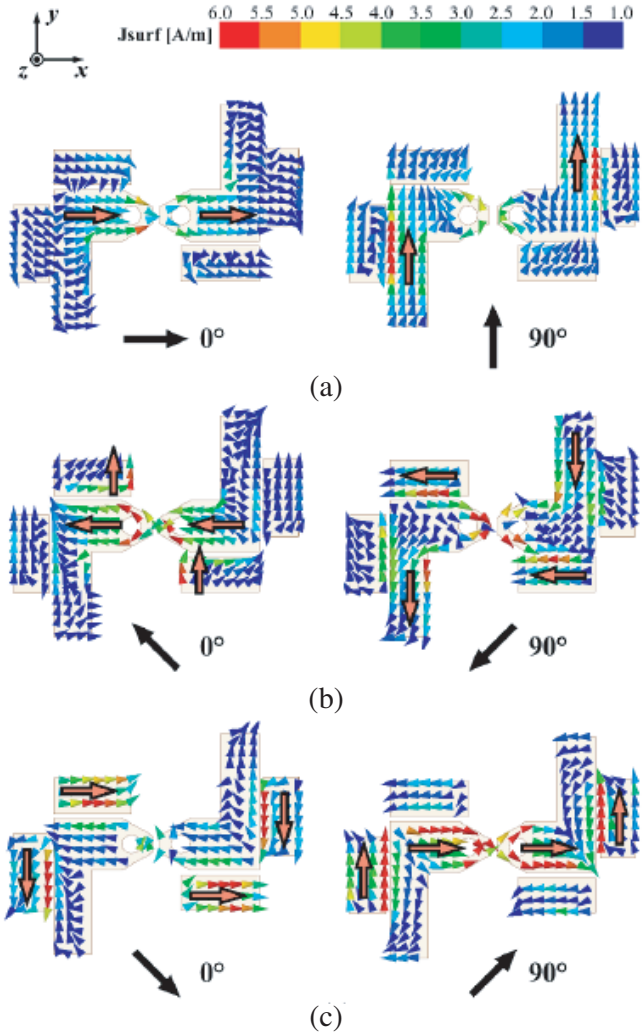

Figure 5. Surface current distributions of the proposed antenna at (a) 1.8 GHz, (b) 2.6 GHz, and (c) 3.1 GHz.

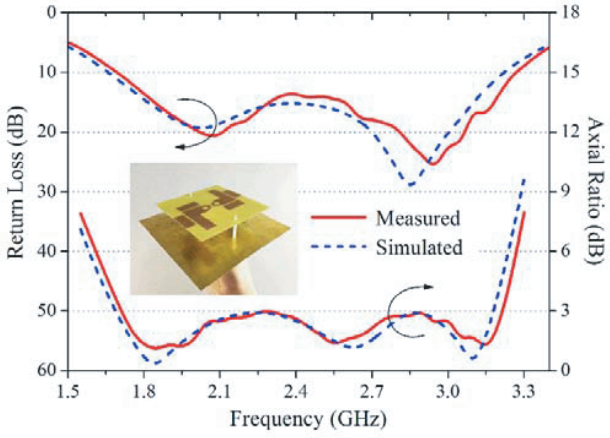

Figure 6. Measured and simulated return loss and axial ratio for the proposed antenna.

3. RESULTS AND DISCUSSION

To validate the design concept, an antenna prototype has been fabricated and tested. The measured return loss and AR at $+z$ direction are presented in Figure 6 with the corresponding simulated results. It can be seen that the measured impedance bandwidth (for return loss > 10 dB) was 64.0% from 1.69 to 3.28 GHz, and desirable measured AR bandwidth (for AR < 3 dB) of 61.3% from 1.71 to 3.22 GHz was

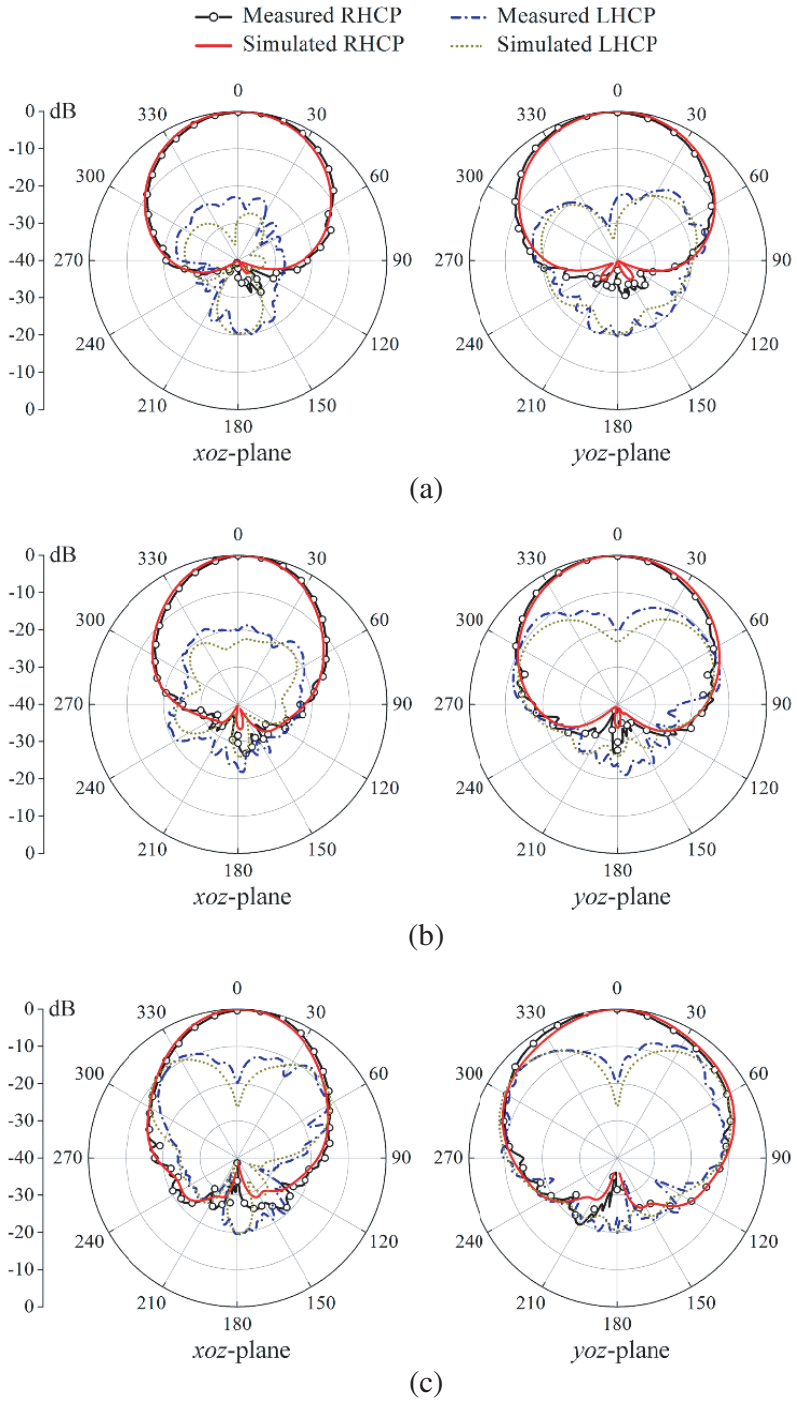

Figure 7. Measured and simulated normalized radiation patterns at (a) 1.8 GHz, (b) 2.6 GHz, (c) 3.1 GHz.

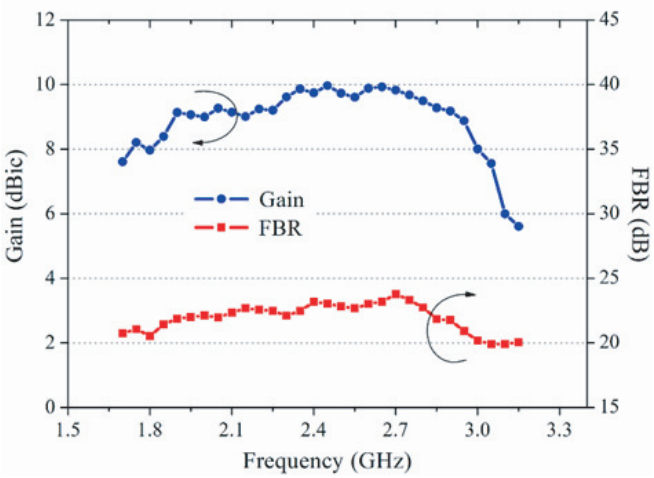

Figure 8. Measured gains and FBRs for the proposed antenna.

Table 1. Comparison of wideband CP antennas.

Ref.	10-dB return loss bandwidth (%)	3-dB axial ratio bandwidth (%)	Gain (dBic)	FBR (dB)	Electrical dimension (λ_0 at center frequency)
[5]	63.6	29.0	about 7.3	> 11	$0.58\lambda_0 \times 0.58\lambda_0 \times 0.22\lambda_0$
[6]	53.0	33.0	1.2–2.7	about 0	$0.53\lambda_0 \times 0.53\lambda_0 \times 0.02\lambda_0$
[7]	57.0	47.8	6.0–7.5	> 14	$0.78\lambda_0 \times 0.78\lambda_0 \times 0.25\lambda_0$
[8]	67.0	60.0	−6.1–7.6	> 15	$1.03\lambda_0 \times 1.03\lambda_0 \times 0.12\lambda_0$
[9]	57.3	41.4	/	> 6	$0.97\lambda_0 \times 0.97\lambda_0 \times 0.52\lambda_0$
[10]	63.3	51.1	about 9.0	> 20	$1.16\lambda_0 \times 1.16\lambda_0 \times 0.24\lambda_0$
Pro.	64.0	61.3	5.6–9.8	> 20	$1.41\lambda_0 \times 1.41\lambda_0 \times 0.25\lambda_0$

also achieved. The experimental data agree reasonably with the simulated results. Subtle differences would be owing to soldering effect of the printed balun and minor fabrication tolerance. Figure 7 shows the simulated and measured far-field radiation patterns, including *xoz*- and *yoz*-planes, at 1.8, 2.6 and 3.1 GHz, respectively. We can conclude from the figure that the antenna features symmetrical and unidirectional RHCP patterns over the operating band. As shown in Figure 8, the measured antenna gains are between 5.6 and 9.8 dBic over the band of interest (1.71–3.22 GHz), and desired front-to-back ratios (FBRs) of better than 20 dB are also obtained.

The comparisons of the measured performances between the proposed antenna and those previously reported antennas [5–10] are listed in Table 1. It is worth noting that the proposed antenna has wider impedance bandwidth and AR bandwidth than the other referenced designs except for the design in [8]. However, antenna gains in [8] fluctuate dramatically (−6.1–7.6 dBic) across the working band. By contrast, the proposed wideband CP antenna exhibits high and stable gains over the entire band.

4. CONCLUSION

A broadband circularly polarized slot-loaded dipole antenna with L-shaped arms and parasitic patches is proposed and studied in this paper. By introducing two pairs of parasitic patches, the modified dipole can yield additional minimum AR points to extend the AR bandwidth effectively. Besides, a pair of circular slots is applied in the dipole arm design to further improve impedance matching and CP performance. The measured results indicate that the proposed antenna not only achieves a 3-dB AR bandwidth of 61.3% within 10-dB return loss bandwidth of 64.0%, but also exhibits stable radiation patterns with antenna gain over 5.6 dBic, and it is a good candidate for broadband CP wireless communication applications.

ACKNOWLEDGMENT

This work was supported by the National Natural Science Foundation of China (Grant No. 61501340).

REFERENCES

1. Nasimuddin, X. M. Qing, and Z. N. Chen, "Compact asymmetric-slit microstrip antennas for circular polarization," *IEEE Trans. Antennas Propag.*, Vol. 59, 285–288, 2011.
2. Ding, K., T. Yu, and Q. Zhang, "A compact stacked circularly polarized annular-ring microstrip antenna for GPS applications," *Progress In Electromagnetics Research Letters*, Vol. 40, 171–179, 2013.
3. Kumar, S., B. K. Kanaujia, A. Sharma, M. K. Khandelwal, and A. K. Gautam, "Single-feed cross-slot loaded compact circularly polarized microstrip antenna for indoor WLAN applications," *Microw. Opt. Technol. Lett.*, Vol. 56, 1313–1317, 2014.
4. Liu, J. C., B. H. Zeng, L. Badjie, S. Drammeh, S. S. Bor, T. F. Hung, and D. C. Chang, "Single-feed circularly polarized aperture-coupled stack antenna with dual-mode square loop radiator," *IEEE Antennas Wireless Propog. Lett.*, Vol. 9, 887–890, 2010.
5. Yang, Z., X. H. Wang, L. Kang, H. Wang, J. Bao, and X.-W. Shi, "A broadband circularly polarized antenna based on cross-dipoles," *Progress In Electromagnetics Research Letters*, Vol. 62, 91–96, 2016.
6. Chang, T. N. and J. M. Lin, "Circularly polarized antenna having two linked slot-rings," *IEEE Trans. Antennas Propag.*, Vol. 59, 3057–3060, 2011.
7. Yang, S. L. S., A. A. Kishk, and K. F. Lee, "Wideband circularly polarized antenna with L-shaped slot," *IEEE Trans. Antennas Propag.*, Vol. 56, 1780–1783, 2008.
8. Guo, Y. X., L. Bian, and X. Q. Shi, "Broadband circularly polarized annular-ring microstrip antenna," *IEEE Trans. Antennas Propag.*, Vol. 57, 2474–2477, 2009.
9. Hu, Y. J., Z. M. Qiu, B. Yang, S. J. Shi, and J. J. Yang, "Design of novel wideband circularly polarized antenna based on Vivaldi antenna structure," *IEEE Antennas Wireless Propog. Lett.*, Vol. 14, 1662–1665, 2015.
10. Hu, W., Z. Y. Tang, P. Fei, and Y. Z. Yin, "Broadband circularly polarized Z-shaped dipole antenna with parasitic strips," *Int. J. RF Microwave Comput. Aided Eng.*, Vol. 27, 2017.